# Enhanced TOF−SIMS Imaging of a Micropatterned Protein by Stable Isotope Protein Labeling

**ARTICLE** *in* ANALYTICAL CHEMISTRY · FEBRUARY 2001

Impact Factor: 5.64 · DOI: 10.1021/ac000771l · Source: PubMed



**4 AUTHORS**, INCLUDING:

Zhongping Yang
Medtronic
**29** PUBLICATIONS **958** CITATIONS
SEE PROFILE

Ashutosh Chilkoti
Duke University
**292** PUBLICATIONS **15,023** CITATIONS
SEE PROFILE

*Anal. Chem.* **2001,** *73,* 143−150

*Accelerated Articles*

# Enhanced TOF-SIMS Imaging of a Micropatterned Protein by Stable Isotope Protein Labeling

Anna M. Belu,[†] Zhongping Yang,[‡] Ryan Aslami,[‡] and Ashutosh Chilkoti*[,‡]

*Physical Electronics, 6509 Flying Cloud Drive, Eden Prairie, Minnesota 55344, and Department of Biomedical Engineering, Box 90281, Duke University, Durham, North Carolina 27708*

**Patterning of biomolecules on surfaces is an increasingly important technological goal. Because the fabrication of biomolecule arrays often involves stepwise, spatially resolved derivatization of surfaces, spectroscopic imaging of these arrays is important in their fabrication and optimization. Although imaging time-of-flight secondary ion mass spectrometry (TOF-SIMS) is a powerful method for spatially resolved surface analysis, TOF-SIMS images of micropatterned proteins on organic substrates can be difficult to acquire, because of the lack of high intensity, protein-specific molecular ions that are essential for imaging under static conditions. In contrast, low-mass ions are of suitable intensity for imaging, but can originate from different chemical species on the surface. A potential solution to this problem is to utilize stable isotope labeled proteins, an approach that has heretofore not been explored in TOF-SIMS imaging of micropatterned proteins and peptides. To investigate the feasibility of stable isotope enhanced TOF-SIMS imaging of proteins, we synthesized $^{15}$N-labeled streptavidin by labeling of the protein during expression from a recombinant gene. The spatial distribution of streptavidin bound to biotin micropatterns, fabricated on a polymer and on a self-assembled monolayer on gold, was imaged by TOF-SIMS. Imaging of high-intensity, low-$m/z$ secondary ions (e.g., $C^{15}N^-$) unique to streptavidin enabled unambiguous spatial mapping of the micropatterned protein with a lateral resolution of a few micrometers. TOF-SIMS imaging of micropatterned $^{15}$N-labeled streptavidin also illustrated the exquisite sensitivity of TOF-SIMS to low fractional coverage of protein (5 Å effective thickness) in the background regions of the protein micropattern.**

The patterning of biomolecules on surfaces is an increasingly important technological goal. Micropatterned proteins and DNA (i.e., patterned with a lateral resolution of 1−100 $\mu$m) are useful for multianalyte sensing, as biomaterial substrates, and as genomic arrays.[1] Because the fabrication of biomolecule arrays often involves stepwise, spatially resolved derivatization of surfaces, spectroscopic imaging of these arrays is important in their fabrication and optimization. Fluorescence microscopy is currently the most commonly used technique to image fluorescently labeled protein and DNA patterns.[2] Although fluorescence microscopy has a number of attractive features, such as its wide availability and its ease of use, it also has a number of limitations. These limitations of fluorescence microscopy are the following: (1) the patterned species has to be labeled with a fluorophore, which can compromise protein function; (2) it is unable to provide chemical or structural information at each stage of the patterning process; (3) it does not provide quantitative information on protein coverage and pattern contrast; and (4) distance-dependent fluorescence quenching of fluorophores on metal substrates further complicates interpretation of the observed protein pattern.[3]

A number of other imaging techniques, in principle, are capable of providing molecular level information about the chemistry and structure of biomolecule arrays. Optical imaging methods such as imaging ellipsometry[4] and surface plasmon microscopy[5] provide

* To whom correspondence should be addressed: (tel) (919) 660-5373; (fax) (919) 660−5362; (e-mail) chilkoti@duke.edu.

† Physical Electronics.

‡ Duke University.

(1) Blawas, A. S.; Reichert, W. M. *Biomaterials* **1998**, *19*, 595−609. Mrksich, M.; Whitesides, G. M. *Trends. Biotechnol.* **1995**, *13*, 228−235. Kumar, A.; Abbott, N.; Kim, E.; Biebuyck, H.; Whitesides. G. M. *Acc. Chem. Res.* **1995**, *28*, 219−226. Xia, Y.; Whitesides, G. M. *Angew. Chem., Int. Ed. Engl.* **1998**, *37*, 551−575.

(2) Lahiri, J.; Ostuni, E.; Whitesides, G. M. *Langmuir* **1999,** *15*, 2055−2060. Vaidya, R.; Tender, L. M.; Bradley, G.; O'Brien, M. J., II; Cone, M.; Lopez, G. P. *Biotechnol. Prog.* **1998,** *14*, 371−377. Nowall, W. B.; Dontha, N.; Kuhr, W. G. *Biosensors Bioelectron.* **1998,** *13*, 1237−1244. Liu, J.; Hlady, V. *Colloids Surf. B* **1996**, *8*, 25−37.

(3) Enderlein, J. *Chem. Phys.* **1999**, *247*, 1−9.

(4) Arwin, H. *Thin Solid Films* **1998**, *13*, 764−774. Jin G.; Jansson, R.; Arwin, H. *Rev. Sci. Instrum.* **1996**, *67*, 2930−2936. Jin, G.; Tengvall, P.; Lundstrom, I.; Arwin, H. *Anal. Biochem.* **1995**, *232*, 69−72.

10.1021/ac000771l CCC: $20.00 
Published on Web 12/08/2000

a quantitative image of the film thickness or coverage density but are insensitive to the different chemical species that are present on the surface. Scanning probe microscopy is exquisitely sensitive to nanometer-scale topography[6] but is only capable of indirectly inferring chemical variations on the surface though lateral force[7] or phase imaging.[8] Recently, imaging X-ray photoelectron spectroscopy has been commercially developed,[9] but both its lateral resolution and its ability to provide molecular information are still untested for insulators. Of the currently available spectroscopic imaging techniques for insulators, time-of-flight secondary ion mass spectrometry (TOF-SIMS) imaging is clearly a powerful method to characterize biomolecular patterns on solid substrates. This is because TOF-SIMS has femtomole-to-attomole sensitivity for organic molecules and enables spatially resolved maps of secondary ions to be simultaneously acquired from the top 10−20 Å of the surface with submicrometer lateral resolution.[10] The spatial distribution and relative concentration of the biomolecule of interest and other chemical species (e.g., residual reactants, contaminants etc.) introduced in the patterning process can therefore be determined by TOF-SIMS.

Recent studies in our laboratory and by other investigators suggest, however, that spatial imaging of protein micropatterns on organic substrates, such as self-assembled monolayers (SAMs) and polymers, by TOF-SIMS is limited by at least two factors.[11] First, organic molecules, including proteins, do not frequently give rise to unique molecular ions with an absolute intensity that is sufficiently large to permit imaging below the static SIMS limit. Second, atomic ions created from the protein pattern often have high enough intensity for TOF-SIMS imaging under static conditions, but they are not unique to the protein; they can be created from the underlying substrate as well as from other organic moieties that are typically introduced during chemical conjugation or binding of the protein to the substrate.

A potential solution to the problems encountered in TOF-SIMS imaging of protein patterns on organic substrates is to use a protein-specific label to discriminate the protein from the underlying substrate. Although stable isotope labeling of proteins is commonly used to determine protein structure and dynamics by solution nuclear magnetic resonance spectroscopy,[12] as well as in mass spectrometry of proteins,[13] its use in static SIMS is less common. Stable isotope labeling has been previously used to decipher the complex surface chemistry of organic plasma deposited thin films,[14] to elucidate the SIMS fragmentation mechanism of a number of synthetic polymers,[15] and to quantitate the concentration of functional groups.[16] To our knowledge, however, the use of stable isotope labeling for TOF-SIMS imaging of micropatterned proteins has not been previously reported.

Stable isotope labeling of proteins is attractive for TOF-SIMS for the following reasons. First, it provides a unique mass label for the protein at the protein expression level and therefore does not require any postexpression, covalent modification of the protein. Second, stable isotope labeling does not typically affect protein structure or function, unlike covalent conjugation of bulky, hydrophobic fluorophores, which can compromise protein function. Third, stable isotope labeling is easily achieved: recombinant DNA techniques now permit the facile cloning or synthesis of the gene encoding a protein of interest.[17] Heterologous expression of the gene from a suitable vector in a host organism, under conditions where the nutrients are stable isotope labeled, then provides a convenient method to synthesize labeled protein with a high degree of isotopic substitution. Finally, stable isotope labeling offers considerable flexibility in the amino acids that are labeled; a protein can be homogeneously labeled by isotopic substitution of a specific atom (e.g., N and C) throughout the protein, or alternatively, specific amino acids can be labeled in the protein.[18]

We report here TOF-SIMS imaging of stable isotope-labeled protein micropatterns and demonstrate that isotopically unique


(5) Rothenhausler, B.; Knoll, W. *Nature* **1988**, *332*, 615−617. Knoll, W.; Zizlsperger, M.; Liebermann. T.; Arnold, S.; Badia, A.; Liley, M.; Piscevic, D.; Schmitt, F. J.; Spinke, *J. Colloids Surf. A.* **2000**, *161*, 115−137. Kambhampati, D. K.; Knoll, W. *Curr. Opin. Colloid Interface Sci.* **1999**, *4*, 273−280. Frutos, A. G.; Brockman, J. M.; Corn, R. M. *Langmuir* **2000**, *16*, 2192−2197. Steiner, G.; Sablinskas, V.; Hubner, A.; Kuhne, C.; Salzer, R. *J. Mol. Struct.* **1999**, *509*, 265−273. Evans, S. D.; Allinson H.; Boden, N.; Flynn, T. M.; Henderson, J. R. *J. Phys. Chem. B* **1997**, *101*, 2143−2148. Thiel, A. J.; Frutos A. G.; Jordan, C. E.; Corn, R. M.; Smith, L. M. *Anal. Chem.* **1997**, *69*, 4948−4956. Jordan, C. E.; Corn, R. M. *Anal. Chem.* **1997**, *69*, 1449−1456. Nelson, B. P.; Frutos, A. G.; Brockman, J. M.; Corn, R. M. *Anal. Chem.* **1999**, *71*, 3928−3934. Jordan, C. E.; Frutos, A. G.; Thiel, A. J.; Corn, R. M. *Anal. Chem.* **1997**, *69*, 4939−4947.

(6) Wadu-Mesthrige, K.; Xu, S.; Amro, N. A.; Liu G. Y. *Langmuir* **1999**, *15*, 8580−8583. Mazzola, L. T.; Fodor, S. P. A. *Biophys. J.* **1995**, *68*, 1653−1660.

(7) Utriainen, M.; Leijala, A.; Niinisto. L.; Matero, R. *Anal. Chem.* **1999**, *71*, 2452−2458. Dupont-Gillain, C. C.; Nysten, B.; Hlady, V.; Rouxhet, P. G. *J. Colloid Interface Sci.* **1999**, *220*, 163−169.

(8) Yip, C. M.; Brader. M. L.; Frank, B. H.; Defelippis, M. R.; Ward, M. D. *Biophys. J.* **2000**, *78*, 466−473. Raghavan, D.; Gu, X.; Nguyen, T.; Vanlandingham, M.; Karim, A. *Macromolecules* **2000** *33*, 2573−2583.

(9) Fulghum, J. E. *J. Electron. Spectrosc. Relat. Phenom.* **1999**, *100*, 331−355. Drummond, I. W. *Philos. Trans. R. Soc. London Ser. A.* **1996**, *354*, 2667−2682. Forsyth, N. M.; Coxon, P. *Surf. Interface Anal.* **1994**, *21*, 430.

(10) Van Vaeck, L.; Adriaens, A.; Gijbels, R. *Mass Spectrom. Rev.* **1999**, *18*, 1−47. Adriaens, A.; Van Vaeck, L.; Adams, F. *Mass Spectrom. Rev.* **1999**, *18*, 48−81. Benninghoven, A. *Angew. Chem., Int. Ed. Engl.* **1994**, *33*, 1023−1043. Hagenhoff. B. *Mikrochim. Acta* **2000**, *132*, 259−271. Odom, R. W. *Appl. Spectrosc. Rev.* **1994**, *29*, 67−116.

(11) Yang, Z.-P.; Belu, A. M.; Sugg, H. W.; Liebmann-Vinson, A.; Chilkoti, A. *Langmuir* **2000,** *16***,** 7482−7492. Hagenhoff, B. *Biosens. Bioelectron.* **1995**, *10*, 885−894. Cannon, D. M.; Pacholski, M. L.; Winograd, N.; Ewing. A. *J. Am. Chem. Soc.* **2000**, *122*, 603−610. Pacholski M. L.; Winograd, N. *Chem. Rev.* **1999**, *99*, 2977−3005. Léonard, D.; Mathieu, H. J. *Fresenius J. Anal. Chem.* **1999**, *365*, 3−11. Makholiso, S. A.; Léonard, D.; Giovangrandi, L.; Mathieu, H. J.; Illegems, M.; Aebischer, P. *Langmuir* **1999**, *15*, 2940−2946. Chevolot, Y.; Bucher, O.; Léonard, D.; Mathieu, H. J.; Sigrist, H. *Bioconj. Chem.* **1999**, *10*, 169−175. Léonard, D.; Chevolot, Y.; Bucher, O.; Haenni, W.; Sigrist, H.; Mathieu, H. J. *Surf. Interface Anal.* **1998**, *26*, 793−799.

(12) Cooke, R. M. *Curr. Opin Chem. Biol.* **1997**, *1*, 359−364. Wang, A. J.; Englander, S. W. *Curr. Opin. Biotechnol.* **1996**, *7*, 403−408. Wagner, G.; Thanabal, V.; Stockman, B. J.; Peng, J. W.; Nirmala, N. R.; Hyberts, S. G.; Goldberg, M. S.; Detlefsen, D. J.; Clubb, R. T.; Adler, M. *Biopolym.* **1992**, *32*, 381−390. Muchmore, D. C.; Mcintosh, L. P.; Russell, C. B.; Anderson, D. E.; Dahlquist, F. W. *Methods Enzymol.* **1989**, *177*, 44−73.

(13) Kelleher, N. L.; Nicewonger, R. B.; Begley, T. P.; McLafferty, F. W. *J. Biol. Chem.* **1997**, *272*, 32215−32220. Chowdhury, S. K.; Vavra, K. J.; Brake, P. G.; Banks, T.; Falvo J.; Wahl, R.; Eshraghi, J.; Gonyea, G.; Chait, B. T.; Vestal, C. H. *Rapid Commun. Mass Spectrom.* **1995**, *9*, 563−569.

(14) Chilkoti, A.; Ratner B. D.; Briggs, D. *Anal. Chem.* **1991**, *63*, 1612−1620. Chilkoti, A.; Ratner, B. D.; Briggs, D. *J. Polym. Sci. Polym. Chem.* **1992**, *30*, 1261−1278.

(15) Vanden Eynde, X.; Reihs, K.; Bertrand, P. *Macromolecules* **1999**, *32*, 2925−2934. Chilkoti, A.; Castner, D. G.; Ratner, B. D. *Appl. Spectrosc.* **1991**, *45*, 209−217.

(16) Briggs, D.; Munro, H. S. *Polym Commun.* **1987**, *28*, 307−309.

(17) Ausubel, F. M.; Brent, R.; Kingston, R. E.; Moore, D. H.; Seidman, J. G.; Smith, J. A.; Struhl, K. *Current Protocols in Molecular Biology*; John Wiley & Sons: New York, 1995.

(18) Kigawa, T.; Muto, Y.; Yokoyama, S. *J. Biomol. NMR* **1995**, *6*, 129−134. Chen, X.; Smith, L. M.; Bradbury, E. M. *Anal. Chem.* **2000**, *72*, 1134−1143.

secondary ions arising from the protein permit unambiguous spatial mapping of the micropatterned protein and enable quantitative determination of the relative contrast between patterned regions and background. We illustrate the enhanced imaging of micropatterned $^{15}$N-labeled streptavidin, especially the clear discrimination of protein against organic background, using two different patterning methods and substrates—microstamping on an activated polymer surface (MAPS)[19] and light-activated micropatterning (LAMP) onto a SAM on gold.[20]

## EXPERIMENTAL SECTION

**Gene Synthesis of Core Streptavidin.** Our gene design for streptavidin is similar to those described previously.[21] Briefly, a synthetic gene for core streptavidin, encoding residues 13−139 of wild-type streptavidin,[22] was designed by reverse transcription using preferred *Escherichia coli* codons and then modified to introduce restriction endonuclease recognition sites for cloning and cassette mutagenesis. *Eco*RI and *Hind*III recognition sites were added to the 5′ and 3′ ends respectively of the gene, to enable ligation of the synthetic gene into pUC19 plasmid (NEB Inc.). An *Nde*I site was also included at the 5′ end, downstream of the *Eco*RI recognition site to allow subsequent insertion of the streptavidin gene into the pET25b expression vector (Novagen Inc.) as well as to provide the initiating methionine codon.

Standard molecular biology protocols were used for the synthesis of the core streptavidin gene.[17] Chemically synthesized oligonucleotides (Integrated DNA Technologies) corresponding to the designed sequence were annealed in solution, ligated into linearized, dephosphorylated, pUC19 (NEB Inc.), and the ligation product was then transformed into XL1 Blue *E. coli* cells. Ligation of the core streptavidin gene into pUC19 was confirmed by DNA sequencing using dye terminator chemistry (ABI 373 fluorescent sequencer, PE Biosystems). The gene was then subcloned into the expression vector pET25b (Novagen Inc.) to yield the expression vector pSTREP and transformed into the BL21(DE3) strain of *E. coli* (Novagen Inc.).

**Expression and Labeling of Recombinant Streptavidin.** BL21(DE3) (Novagen Inc.) cells transformed with pSTREP were cultured overnight in 50 mL of Circlegrow liquid media (Bio 101 Inc.) supplemented with ampicillin (100 $\mu$g/mL), at 37 °C. The cells were centrifuged, resuspended in 5 mL of fresh Circlegrow medium containing 100 $\mu$g/mL ampicillin, and 3 mL of the resuspended culture was used to inoculate 1 L of Circlegrow medium supplemented with 100 $\mu$g/mL ampicillin in shaker flasks. The culture was incubated with shaking at 37 °C until the absorbance at 600 nm reached 0.8, at which time the cells were removed, pelleted at 3000*g*, resuspended in M9 minimal media containing $^{15}NH_4Cl$ as the sole nitrogen source, and isopropyl $\beta$-D-thiogalactopyranoside (IPTG) was added (1 mM) to induce protein expression. Nonisotopically labeled streptavidin was produced without switching the media from Circlegrow media to minimal media prior to induction, and the 1-L culture was allowed to reach an OD of 0.8, at which protein expression was induced by adding IPTG to a final concentration of 1 mM. Cells were cultured for a further 5 h (3 h for nonisotopically labeled protein expression), after which they were harvested by centrifugation at 3000*g* for 15 min. The cell pellets were stored at −70 °C till further use.

**Purification of Labeled Protein.** The frozen cell pellet was resuspended and thawed in 50 mL of lysis buffer (50 mM Tris, 200 mM NaCl, 5 mM EDTA, 8% (w/v) sucrose, 1 mM phenylmethanesulfonyl fluoride, 2% (v/v) Triton X-100, pH 8.0). The cells were lysed by repeated rounds of sonication (Sonic Dismembrator 550, Fisher Scientific). Because streptavidin is sequestered in insoluble inclusion bodies in *E. coli* upon overexpression,[21] the insoluble fraction of the cell lysate, containing the inclusion bodies, were washed in Triton X-100 and then dissolved overnight in 50 mL of 6 M guanidine hydrochloride. The solubilized protein was then dialyzed overnight against 20 L of 50 mM Tris, 8 mM EDTA, 100 mM NaCl, pH 7.9. The dialysis buffer was exchanged twice over 24 h. Insoluble protein was removed by centrifugation, and the refolded protein was then concentrated by ultrafiltration and purified by iminobiotin affinity chromatography.[23] The yield of $^{15}$N-labeled streptavidin was ∼2 mg/L of culture.

**Electrospray Ionization Mass Spectrometry (ESI-MS) of Streptavidin.** ESI-MS was performed on a Perkin-Elmer Sciex API 150EX spectrometer. Samples were infused into the mass spectrometer at a flow rate of 5 $\mu$L/min using a Harvard syringe pump. ESI mass spectra were acquired in the positive ion mode. Observed masses were calculated from the ion signals observed for the protonation charge states of all molecular species, using the program BioMultiview (Sciex). The calculated average mass of $^{15}$N-labeled recombinant streptavidin was 13 435 Da, while the experimentally determined mass was 13 424 Da, which suggested ∼90% $^{15}$N substitution of the nitrogen atoms in the protein.

**Patterning of Streptavidin.** Light-activated micropatterning, details of which have been previously reported elsewhere,[19] was used to create streptavidin patterns on a SAM on gold. Microstamping onto an activated polymer surface, a variant of reactive microcontact printing, was used to patern streptavidin with micrometer lateral resolution onto poly(etheylene terephthalate) (PET).[20] A schematic of both patterning methods is shown in Figure 1, and experimental details are in Supporting Information.

**Time-of-Flight Secondary Ion Mass Spectrometry.** TOF-SIMS spectra and images were obtained on a TRIFT II TOF-SIMS instrument (Physical Electronics, Eden Prairie MN). A mass-filtered $^{69}Ga^+$ liquid metal primary ion gun was used with a current of ∼600 pA. For spectral acquisition, the gun was operated at 15 keV and a pulse width of 12 ns. For imaging, the gun was operated at 25 keV and a pulse width of 30 ns. Details of the spectrometer are described elsewhere.[24] The data were acquired over a mass range of $m/z$ 0−1500. The data were collected using an ion dose below the static SIMS limit of $10^{13}$ ions/cm$^2$.[25] A low-energy electron beam was used for charge compensation on the polymer samples.


(19) Yang, Z.-P.; Chilkoti, A. *Adv. Mater.* **2000**, *12*, 413−417.
(20) Yang, Z.-P.; Frey, W.; Oliver, T.; Chilkoti, A. *Langmuir* **1999**, *16*, 1751−1758.
(21) Thompson, L.; Weber, P. C. *Gene* **1993**, *136*, 243−246. Sano, T. Cantor, C. R. *Proc. Natl. Acad. Sci. U.S.A.* **1990**, *87*, 142−146. Chilkoti, A.; Tan, P. H.; Stayton, P. S. *Proc. Natl. Acad. Sci. U.S.A.* **1995**, *92*, 1754−1758.
(22) Argarana, C. E.; Kuntz, I. D.; Birken, S.; Axel, R.; Cantor, C. R. *Nucleic Acids Res.* **1986**, *14*, 1871−1882.
(23) Heney, G.; Orr, G. A. *Anal. Biochem.* **1981**, *114*, 92−96. Hoffman, K.; Wood, S. W.; Brinton, C. A.; Montbellier, J. A.; Finn, F. M. *Proc. Natl. Acad. Sci. U.S.A.* **1980**, *77*, 4666−4668.
(24) Schueler, B. *Microsc. Microanal. Microstruct.* **1992**, *3*, 119−139.
(25) Briggs, D.; Wootton, A. B. *Surf. Interface Anal.* **1982**, *4*, 109.

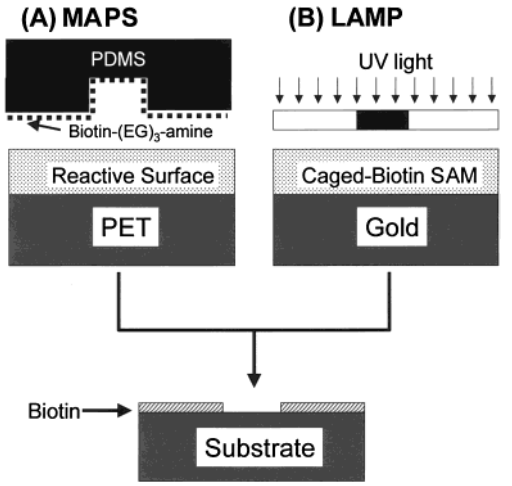


Figure 1. (A) Schematic of MAPS for micropatterning biotin−amine onto a polymer. The polymer surface is homogeneously derivatized from solution to introduce amine-reactive groups. A PDMS stamp, cast from a microfabricated master with micrometer-scale relief features, is inked with biotin−amine and brought into contact with the surface, which results in spatially resolved coupling of biotin to the polymer surface. (B) Schematic of LAMP to photopattern biotin on a SAM on gold: a MeNPOC−biotin−SAM on gold is irradiated with 350−360-nm UV light through a chrome-on-glass photomask, which releases the MeNPOC "caging" group and reconstitutes biotin in the irradiated regions. In both MAPS and LAMP, subsequent incubation of the micropatterned biotin with streptavidin results in the formation of streptavidin micropatterns.

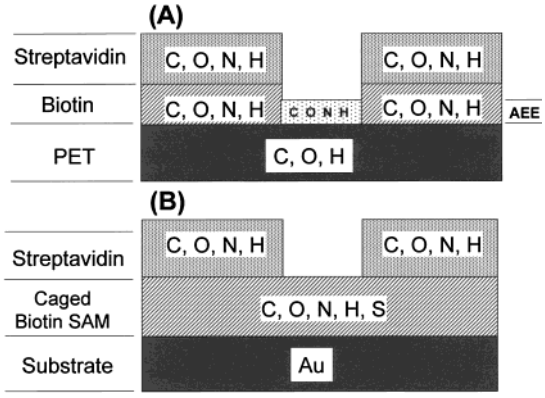


Figure 2. Schematic (cross-sectional view) of streptavidin bound to biotin micropatterns fabricated by (a) MAPS on PET and (b) LAMP on a photolabile "caged" biotin-derivatized SAM on Au. The schematic shows the spatial distribution of atoms across a vertical cross section and illustrates the chemical complexity of these micropatterned surfaces. The thicknesses of the different molecular layers introduced in the patterning by MAPS and LAMP are not to scale. The schematic also assumes that each chemical derivatization step proceeds to completion and that there is no nonspecifically adsorbed protein in the background region.

## RESULTS AND DISCUSSION

The requirements of any protein patterning methodology are that it should enable spatial organization of one or more proteins on a surface at a specified concentration, with controlled orientation, and should achieve high spatial selectivity—contrast—between patterned regions and background[1]. Because the optimal patterning scheme for a given application is likely to be dictated by chemical and structural constraints imposed by the substrate, we have developed a number of complementary methods to micropattern proteins on different substrates (Figure 1). These methods, which employ different spatially resolved coupling strategies are (1) microstamping on an activated polymer surface[19] and (2) light-activated micropatterning of proteins on self-assembled monolayers on gold.[20]

**Micropatterned Streptavidin on PET Fabricated by MAPS.** The surface of PET was chemically derivatized to introduce carboxylic acid groups on the surface of PET, and the carboxylic acid groups were converted to reactive pentafluorophenyl esters by reaction with PFP/EDAC.[19] Subsequently, a PDMS stamp with periodic features of 40-$\mu$m-diameter circles, was inked with an amine-terminated biotin derivative (biotin−amine) (Figure 1A). Making contact of the stamp with the surface resulted in spatially resolved transfer and conjugation of biotin−amine with the reactive esters present on the surface of PET. Subsequent incubation with streptavidin or [$^{15}$N]streptavidin generated streptavidin patterns on the surface, mediated by the high-affinity streptavidin−biotin interaction.[26] The chemical complexity of the surface is illustrated by Figure 2A, which is a schematic of the spatial distribution of the different elements present in a vertical cross section of a PET surface that is micropatterned with streptavidin using MAPS.

To characterize the streptavidin pattern on PET created by MAPS, TOF-SIMS spectra were acquired of streptavidin, homogeneously immobilized on biotin-derivatized PET. The TOF-SIMS spectra of unlabeled and $^{15}$N-labeled streptavidin, both bound to biotin-derivatized PET-COOH (termed PET-biotin) are shown in Figures 3 and 4. Characteristic peaks for unlabeled streptavidin in positive ion TOF-SIMS are observed at $m/z$ 70 ($C_4H_8N^+$) and 130 ($C_9H_8N^+$) (Figure 3A). The spectrum also has peaks characteristic of the PET substrate at $m/z$ 76, 104, 149, 193 $[M + H]^+$, 237, 341, 385 $[2M + H]^+$, 429, and 577 $[3M + H]^+$.[27] In comparison, the spectrum of $^{15}$N-labeled streptavidin bound to biotin-derivatized PET shows a shift in the characteristic streptavidin fragments to 1 $m/z$ higher, at $m/z$ 71 and 131, representing $C_4H_8{}^{15}N^+$ and $C_9H_8{}^{15}N^+$ (Figure 3B). These shifts to 1 $m/z$ higher clearly confirm that the $m/z$ 70 and 130 ions are created from streptavidin and not from adsorbed organic contaminants.

Typically, molecular ions are attractive for TOF-SIMS imaging because they can uniquely identify a specific molecule. The molecular ions at $m/z$ 70 and 130, however, have limited utility for TOF-SIMS imaging of micropatterned streptavidin. This is because of the following reasons. First, these peaks are of low intensity, which makes imaging the spatial distribution of these ions extremely difficult. Longer acquisition times do not improve the signal-to-noise ratio for larger fragments, because the experiment goes beyond the "static SIMS limit", where the flux of primary ions becomes so high that the molecules themselves are destroyed before analysis.[25] We maintained the static SIMS limit in the imaging experiments because we wanted to sample the top 10−20 Å. This is an important experimental consideration because all the chemical information is contained in this depth. Second, these ions are generic, because they are fragmentation products

(26) Wilchek, M.; Bayer, E. *Avidin−Biotin Technology*; Methods in Enzymology 184; Academic Press: San Diego, 1990.

(27) The Static SIMS Library, Version 2, SurfaceSpectra Ltd., Manchester, U.K., 1999. Briggs, D. *Surf. Interface Anal.* **1986**, *8*, 133−136.

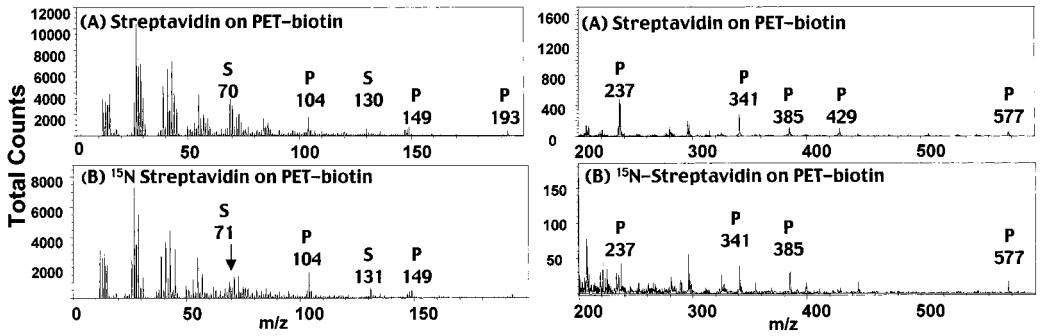


Figure 3. (+) TOF-SIMS spectrum of streptavidin bound to PET-biotin: (A) unlabeled streptavidin; (B) $^{15}$N-labeled streptavidin. Characteristic streptavidin peaks are labeled S. Characteristic PET peaks are labeled P.

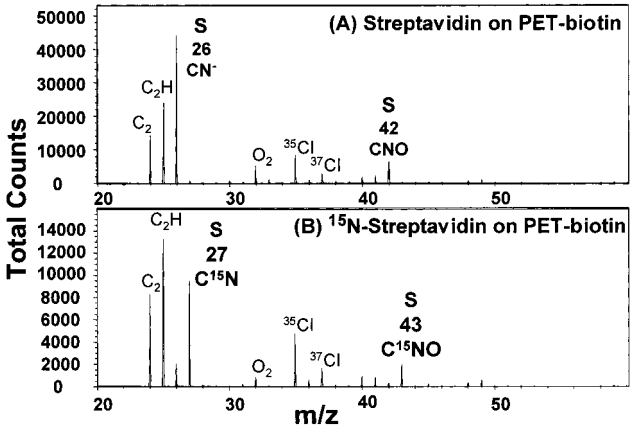


Figure 4. (−) TOF-SIMS spectrum of streptavidin bound to PET-biotin: (A) unlabeled streptavidin; (B) $^{15}$N-labeled streptavidin. Characteristic streptavidin peaks are labeled S. Characteristic PET peaks are labeled P.

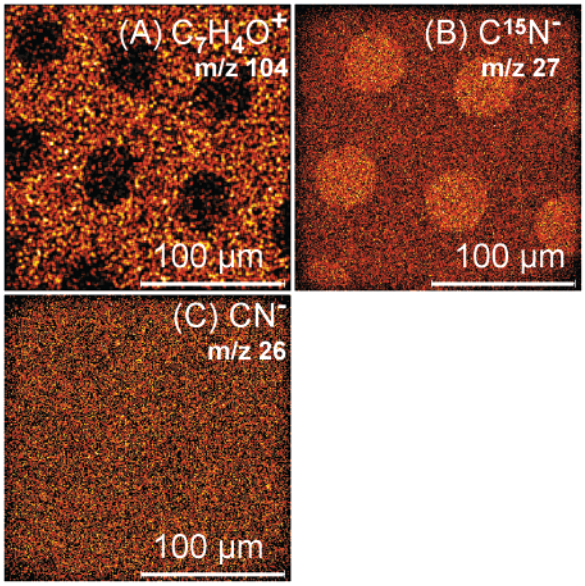


Figure 5. TOF-SIMS images (200 × 200 $\mu$m) of $^{15}$N-labeled streptavidin bound to a biotin micropattern fabricated by MAPS: (A) *m*/*z* 104 ($C_7H_4O^+$); (B) *m*/*z* 27 ($C^{15}N^-$); (C) *m*/*z* 26 ($CN^-$). The *m*/*z* 27 anion is unique to the protein and enables unambiguous imaging of the spatial distribution of streptavidin.

of the polypeptide backbone. Mantus et al. showed that these ions are created from Pro, Arg (*m*/*z* 70), and Trp residues (*m*/*z* 130), which are typically present in most proteins.[28] In protein immobilization and micropatterning using affinity interactions such as the streptavidin−biotin pair, proteins such as BSA and casein are often added as blocking agents to the protein binding buffer to prevent nonspecific adsorption of streptavidin to the surface.[29] Because molecular ions, such as $C_3H_8N^+$ and $C_4H_{11}N^+$, are emitted by many proteins under primary ion bombardment, they do not allow streptavidin to be uniquely discriminated on the basis of these ions, especially if protein-based blocking agents are used during patterning.

In negative ion TOF-SIMS, characteristic peaks for streptavidin are observed at *m*/*z* 26 ($CN^-$) and 42 ($CNO^-$) (Figure 4A). Unique molecular anions are not observed. The negative ion spectrum of $^{15}$N-labeled streptavidin shows a corresponding shift in nitrogen-containing streptavidin fragments to 1 *m*/*z* higher, at *m*/*z* 27 and 43, representing $C^{15}N$ and $C^{15}NO$ (Figure 4B). The peaks at *m*/*z* 27 and 43 for $^{15}$N-labeled streptavidin ($C^{15}NO^-$ and $C^{15}NO^-$, respectively) are especially important in negative mode because they are created primarily from the protein and have a large enough absolute intensity to enable imaging of the protein within the static SIMS limit. We note an *m*/*z* 27 anion with much lower intensity is observed for unlabeled streptavidin bound to biotin-derivatized PET, which arises from the natural isotope distribution of $C^{15}N^-$ and $^{13}CN^-$ and, possibly, from $C_2H_3^-$ and $CHN^-$.

Peaks that are characteristic of each molecular species present on the surface were used to map the distribution of that species by imaging TOF-SIMS (Figure 5). The image of the characteristic PET fragment (*m*/*z* 104, $C_7H_4O^+$) shows higher signal intensity in the regions that were not in contact with the stamp (Figure 5A). Although PET is present throughout the field of view, the intensity of the *m*/*z* 104 cation is lower in the patterned regions. This is because the higher coverage of bound streptavidin in the patterned regions decreases the absolute intensity of PET-specific ions, which is consistent with the ~20-Å sampling depth of TOF-SIMS.[30]

The image of *m*/*z* 27 ($C^{15}N^-$) indicates preferential streptavidin binding to the biotinylated 40-$\mu$m-diameter circles (Figure 5B), but a lower concentration of streptavidin is clearly observed in

(28) Mantus, D. S.; Ratner, B. D.; Carlson, B. A.; Moulder, J. F. *Anal. Chem.* **1993**, *65*, 1431−1438.

(29) Pruslin, F. H.; To, S. E.; Winston, R.; Rodman, T. C. *J. Immunol. Methods* **1991**, *137*, 27−35. Mohammad, K.; Esen, A. *J. Immunol. Methods* **1989**, *117*, 141−145. Vogt, R. F. Jr.; Phillips, D. L.; Henderson, L. O.; Whitfield, W.; Spierto, F. W. *J. Immunol. Methods* **1987**, *101*, 43−50.

(30) Hagenhoff, B.; Deimel, M.; Benninghoven, A.; Siegmund, H.-U.; Holtkamp, D. *J. Phys. D. Appl. Phys.* **1992** *25*, 818−832.

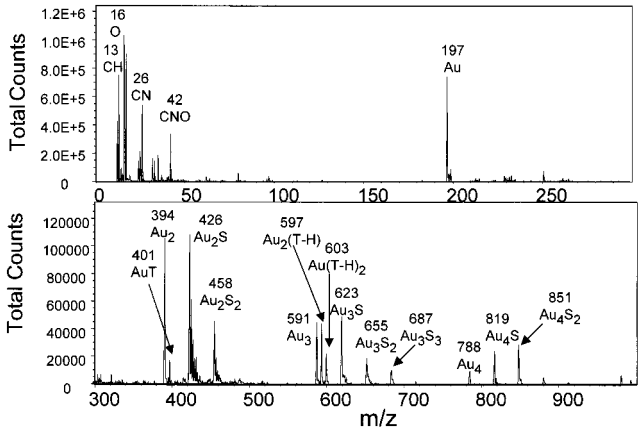


Figure 6. (−) TOF-SIMS spectrum of unlabeled streptavidin bound to UV-irradiated, caged biotin SAM. The $CN^-$ and $CNO^-$ ions can be created from biotin, DADOO, or streptavidin. In the high-mass range, clusters of Au and MUOH are detected (T, MUOH; S, sulfur).

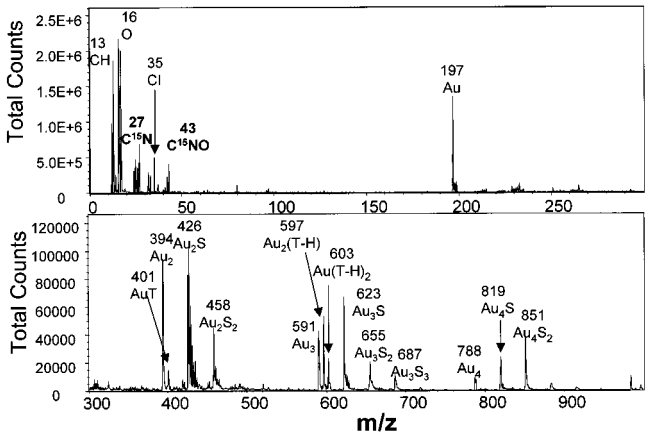


Figure 7. (−) TOF-SIMS spectrum of $^{15}N$-labeled streptavidin bound to a UV-irradiated, caged biotin SAM. The $CN^-$ and $CNO^-$ ions can be created from biotin and DADOO while the $C^{15}N^-$ ion is primarily created from streptavidin. In the high-mass range clusters of Au and MUOH are detected (T, MUOH; S, sulfur).

the regions between the circles, indicating significant nonspecific adsorption of streptavidin to the nonbiotinylated background. $^{15}N$-Labeling of streptavidin is critical in mapping streptavidin, because it provides an intense $m/z$ 27 fragment ($C^{15}N^-$) for the micropatterned protein and thereby permits streptavidin to be distinguished from other species in the sample in TOF-SIMS analysis. Because this fragment is intense, it also allows high signal-to-noise images to be generated within the static SIMS limit.

In contrast, the image of $m/z$ 26 ($CN^-$) in negative ion mode shows a homogeneous distribution of intensity (Figure 5C). The lack of contrast in the $m/z$ 26 is caused by the emission of this fragment from three different molecules present on the surface (Figure 2A): (1) peptide backbone and nitrogen-containing side chains in streptavidin that were not isotopically substituted with $^{15}N$ during labeling of protein during expression, (2) biotin, and (3) AEE.

**Micropatterned Streptavidin on a Mixed COOH/OH-Terminated SAM Fabricated by LAMP.** The second example we chose to illustrate the enhanced TOF-SIMS imaging of proteins that is achieved by $^{15}N$-protein labeling is a photopatterning process—LAMP. In LAMP, homogeneously immobilized, caged biotin on a SAM on gold is irradiated through a photomask, which reconstitutes functional biotin in the irradiated regions[20] (Figure 1B). Subsequently, incubation of the surface with streptavidin results in the formation of a protein pattern. We have previously shown by confocal microscopy that protein micropatterns with ~5-$\mu$m lateral resolution can be fabricated by LAMP.[20] Imaging ellipsometry revealed that the effective layer thickness of streptavidin in the irradiated regions was ~20 Å and that nonspecific adsorption of streptavidin to the background, masked region was ~5 Å, leading to a contrast ratio of 4:1.[20] The elemental distribution in a vertical cross section of the surface of a SAM on gold, patterned with streptavidin by LAMP, is shown in Figure 2B.

The negative TOF-SIMS spectrum of streptavidin bound to a caged biotin-derivatized SAM, after homogeneous UV irradiation of the entire surface at 350 nm for 20 min, is shown in Figure 6. In the low-$m/z$ range, characteristic peaks for streptavidin are observed at $m/z$ 26 ($CN^-$) and 42 ($CNO^-$). In the high-mass range, peaks are observed for Au ($m/z$ 197) and $Au_xS_y$ clusters, which are commonly observed for SAMs on Au.[31] Peaks are also observed for MUOH, which was the major constituent of the binary SAM (90 mol % in solution). The high-mass MUOH−Au clusters are observed at $m/z$ 401, 597, and 603, representing AuT, $Au_2(T-H)$, and $Au(T-H)_2$, respectively, where T represents intact MUOH.[31] Surprisingly, no peaks were observed from the MHA component of the SAM. This is probably because MHA is derivatized with biotin, and subsequent binding of streptavidin prevents desorption of molecular MHA−Au clusters.

Streptavidin labeled with $^{15}N$ bound to the biotin-derivatized mixed SAM was also analyzed by TOF-SIMS. In the negative ion mode (Figure 7), the spectrum is similar to that of unlabeled streptavidin in its signals for Au, $Au_xS_y$, and Au−thiol clusters.[31] Additionally, distinct ions are observed from $^{15}N$-labeled streptavidin at $m/z$ 27 and 43 ($C^{15}N^-$ and $C^{15}NO^-$). The isotopic shifts of +1 $m/z$ compared to unlabeled streptavidin unambiguously identify these ions as arising from streptavidin.

We next examined the binding of streptavidin to a biotin micropattern that was created by LAMP on a mixed SAM. The negative TOF-SIMS images of streptavidin incubated with caged biotin-derivatized SAM, after UV deprotection through a photomask, are shown in Figure 8. The images of $Au^-$ ($m/z$ 197) (Figure 8A) and Au−thiol clusters such as $Au_2(T-H)^-$ (Figure 8B) have higher intensity in the center of the image. The TOF-SIMS image of $CN^-$ at $m/z$ 26 shows distinct contrast inversion (Figure 8C); the central region has lower intensity compared to the top and bottom regions of the image. The $m/z$ 26 anion can be created from streptavidin, biotin, or DADOO. These images indicate that the central region was presumably masked and where biotin was therefore not photodeprotected, while the top and bottom regions were UV irradiated. Loss of the MeNPOC caging group in the irradiated regions results in reconstitution of biotin, and the irradiated regions consequently exhibit a higher coverage of streptavidin upon incubation of the surface with streptavidin, compared to the background, masked regions.

The greater coverage of streptavidin in the upper and lower regions of the sample decreases the emission of Au-specific ions

(31) Offord, D. A.; John, C. M.; Linford, M. R.; Griffin, J. H. *Langmuir* **1994**, *10*, 883−889. Patel, N.; Davies, M. C., Hartshorne, M.; Heaton, R. J.; Roberts, C. J.; Tendler, S. J. B.; Williams, P. M. *Langmuir* **1997**, *13*, 6485−6490.

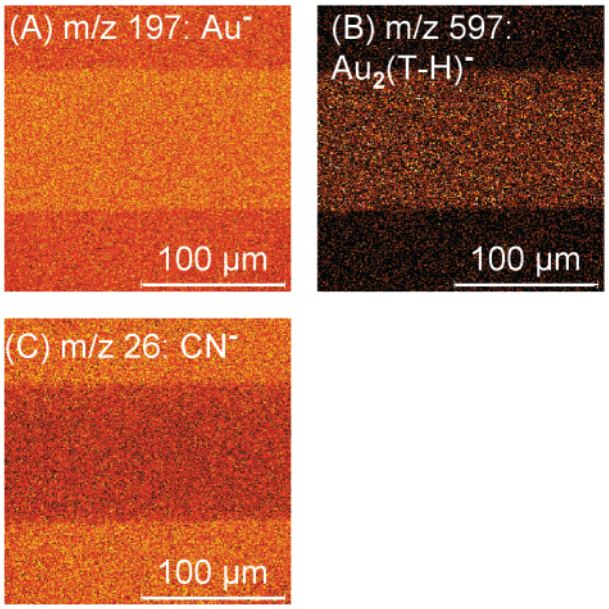


Figure 8. (−) TOF-SIMS images (200 × 200 $\mu$m) of streptavidin, bound to a biotin micropattern fabricated by LAMP. (A) $Au^-$ (*m*/*z* 197); (B) $Au_2(T-H)^-$ (*m*/*z* 597); (C) $CN^-$ (*m*/*z* 26).

because they are buried below the biotin and streptavidin layer and is consistent with the 20−30-Å sampling depth of organic macromolecules in TOF-SIMS.[30] In contrast, the $CN^-$ signal is more intense from the top and bottom regions that were irradiated prior to incubation with streptavidin. Although the $CN^-$ ion can be created from biotin, streptavidin, or the DADOO linker, its higher intensity from the upper and lower regions of the image suggests the preferential localization of streptavidin in the UV-irradiated regions, due to the presence of photoactivated biotin.

The preceding discussion clearly shows that TOF-SIMS imaging only permits the spatial distribution of the protein to be inferred from the observed contrast in the images, because the $CN^-$ ion (*m*/*z* 26) used to map streptavidin can also be generated from three other species on the surface (i.e., MeNPOC-biotin, biotin, and DADOO). Furthermore, no additional information regarding protein coverage in the pattern and background is available from these images because the $CN^-$ ion is not specific to streptavidin.

In comparison, $^{15}N$-isotope labeling of streptavidin greatly simplifies interpretation of TOF-SIMS images of streptavidin, micropatterned by LAMP onto a SAM on Au. Figure 9 shows images of $^{15}N$-labeled streptavidin bound to the photopatterned biotin-derivatized SAM. The negative ion TOF-SIMS image of *m*/*z* 27 ($C^{15}N^-$) clearly shows a higher coverage of streptavidin in the center of the pattern (Figure 9A). The higher intensity of this protein-specific ion from the central, vertical stripe clearly identifies this as the irradiated region with uncaged, active biotin to which streptavidin preferentially binds, mediated by molecular recognition between biotin and streptavidin.

In contrast, the image of *m*/*z* 26 ($CN^-$) has a higher intensity in the adjoining regions (Figure 9B). The *m*/*z* 26 ($CN^-$) ion is created from three species: caged biotin, which is homogeneously immobilized on the surface, the N atoms in streptavidin that were not substituted with $^{15}N$, and the DADOO linker between COOH groups on the SAM and biotin. The lower intensity of this ion

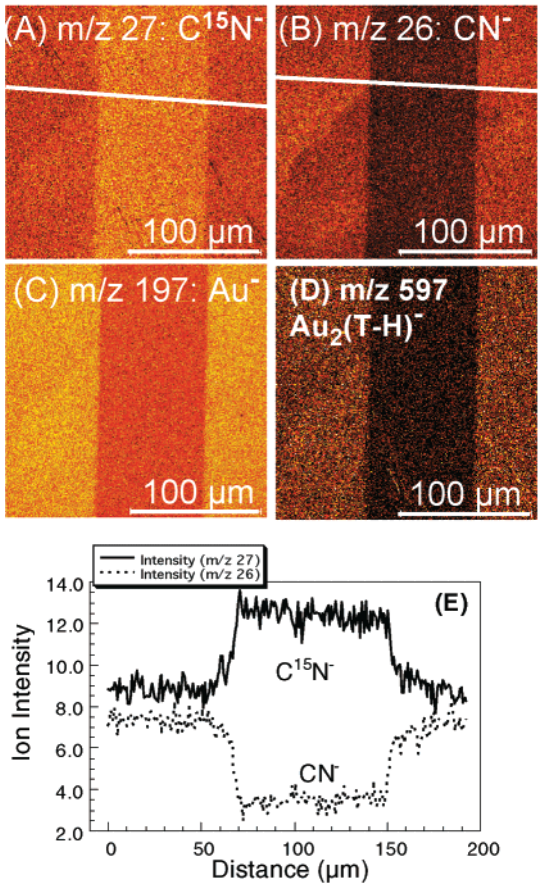


Figure 9. (−) TOF-SIMS images (200 × 200 $\mu$m) of $^{15}N$-labeled streptavidin, bound to a biotin micropattern fabricated by LAMP: (A) $^{15}CN^-$ (*m*/*z* 27); (B) $CN^-$ (*m*/*z* 26); (C) $Au^-$ (*m*/*z* 197); (D) $Au_2(T-H)^-$ (*m*/*z* 597), The spatial distribution of streptavidin is positively identified by the ion intensity of *m*/*z* 27, which is primarily created from the protein ($C^{15}N^-$). (E) Line profiles of absolute ion intensity from images in (A) and (B).

from the central, vertical stripe is consistent with the higher coverage of $^{15}N$-enriched streptavidin in this region. The higher intensity of $Au^-$ (Figure 9C) and Au−MUOH clusters (Figure 9D) also corresponds to the masked regions (i.e., left and right vertical stripes). These results clearly demonstrate that the unique $^{15}N$ label in streptavidin was critical in enabling unambiguous discrimination of streptavidin from other nitrogen-containing species present on the surface.

$^{15}N$ imaging of streptavidin also enabled comparison of the relative concentration of the protein in the pattern with background regions. This was achieved by quantifying the absolute intensity of the $^{15}CN^-$ ion (*m*/*z* 27) over a representative region of the [$^{15}N$]streptavidin pattern (Figure 9E). In comparison, the line intensity profile of $CN^-$ (*m*/*z* 26) for the same sample shows contrast inversion between the pattern and background, because the presence of $^{15}N$-enriched streptavidin decreases the emission efficiency of $CN^-$ ions (created from biotin and DADOO, which are buried below the protein overlayer) from the central region. Although TOF-SIMS cannot provide a quantitative estimate of protein coverage, comparison of the relative intensities in the patterned region with background with the previous imaging ellipsometry results are instructive. We previously determined an effective streptavidin thickness of ∼20 and 5 Å for the irradiated

and masked regions, respectively, assuming a refractive index of 1.45 for a densely packed monolayer such as a two-dimensional protein crystal.[32] The relative intensity of these ions from the background compared to the patterned regions is consistent with the ~20-Å sampling depth of TOF-SIMS. In particular, they clearly show the exquisite sensitivity of TOF-SIMS imaging to quantitating submonolayer coverage (≤5 Å thickness) of a protein against a complex organic substrate.

There are several possible scenarios in which stable isotope labeled biomolecules are likely to be useful for TOF-SIMS imaging of biomolecular patterns. First, in micropatterning a peptide or protein directly onto a substrate by spatially localized adsorption or covalent conjugation, a unique reporter (e.g., $^{15}N$) could be incorporated during solid-phase synthesis of the peptide or during expression of the protein in a suitable host. A second application, which is directly illustrated in this paper, is related to the ubiquitous use of streptavidin as a biomolecular adapter for "affinity patterning". Because streptavidin is a homotetramer with dyad symmetry, patterning of streptavidin onto a biotin pattern provides a universal strategy to fabricate biomolecular patterns, by subsequent incubation of the streptavidin pattern with a biotinylated molecule. The use of stable isotope labeled streptavidin then provides a convenient method to verify the fidelity and quality of the patterned streptavidin template by TOF-SIMS imaging, prior to patterning the biomolecule of interest.

## SUMMARY AND CONCLUSIONS

An important goal in the patterning of biomolecules is to control the surface concentration of the biological ligand in the patterned region, while minimizing nonspecific adsorption or binding of the ligand to the background, unpatterned regions. For example, spatial selectivity is critical in the fabrication of micropatterned biological ligands (e.g., cell adhesive proteins, and peptide ligands) created for cell interaction studies, because cells are exquisitely sensitive to even low surface concentration of biological ligands,[33] and the ability to modulate their behavior by introducing geometrically patterned peptide and protein ligands[34] is likely to depend on sensitive methods to determine the extent of nonspecific adsorption in the background regions. Although ellipsometry and SPR are capable of quantifying the surface density on reflective substrates, they cannot easily provide this information about coverage on more complex, polymeric biomaterials.

In contrast, as shown here, TOF-SIMS imaging of a stable isotope labeled protein pattern enables characterization of its spatial distribution and relative contrast, even against a complex organic background. We have shown that isotopic labeling provides unique protein fragments in the TOF-SIMS spectra and that an isotopically enriched, low-mass fragment provides high-quality images of protein micropatterns with little interference from the other organic species present in the surface region. Finally, TOF-SIMS imaging of micropatterned $^{15}N$-labeled streptavidin also illustrated the exquisite sensitivity of TOF-SIMS to low fractional coverage of protein (5 Å effective thickness) in the background regions of the protein micropattern. The ability to quantify the nonspecific adsorption of protein by the use of stable isotope labeled biomolecules is likely to prove extremely useful in the optimization of micropatterned biofunctionalized surfaces for biomaterial and biosensor applications.

## SUPPORTING INFORMATION AVAILABLE

Experimental details. This material is available free of charge via the Internet at http://pubs.acs.org.

Received for review July 5, 2000. Accepted November 13, 2000.

AC000771L

(32) Darst, S. A.; Ahlers, M.; Meller, P. H.; Kubalek, E. W.; Blankenburg, R.; Ribi, H. O.; Ringsdorf, H.; Kornberg, R. D. *Biophys. J.* **1991**, *59*, 387−396.

(33) Massia, S. P.; Hubbell, J. A. *J. Biomed. Mater. Res.* **1991**, *25*, 223−242. Massia, S. P.; Hubbell, J. A. *J. Cell Biol.* **1991**, *114*, 1089−1100. Hubbell, J. A.; Massia, S. P.; Desai, N. P.; Drumheller, P. D. *Bio/Technol.* **1991**, *9*, 568−572.

(34) Chen, C. S.; Mrksich, M.; Huang, S.; Whitesides, G. M.; Ingber, D. E. *Science* **1997**, *276*, 1425−1428. Mrksich, M.; Dike, L. E.; Tien, J.; Ingber, D. E.; Whitesides, G. M. *Exp. Cell Res.* **1997**, *235*, 305−313. Chen, C. S.; Mrksich, M.; Huang, S.; Whitesides, G. M.; Ingber D. E. *Biotechnol. Prog.* **1998**, *14*, 356−360.